Available online at www.sciencedirect.com

ScienceDirect

IFAC PapersOnLine 52-21 (2019) 51–56

Vent Valve Thrust Force for Surface Effect Ships ⋆

Håkon Teigland * **Vahid Hassani** **,***,[1] **Øyvind Auestad** ****

* *Department of Marine Technology, Norwegian Univ. of Science and Technology, Trondheim, Norway.*

** *Department of Mechanical, Electronics and Chemical Engineering, Oslo Metropolitan University, Oslo, Norway (e-mail: vahid.hassani@oslomet.no).*

*** *Department of Ships and Ocean Structures, SINTEF Ocean, Trondheim, Norway.*

**** *Umoe Mandal AS, Mandal, Vest-Agder, Norway.*

Abstract:
The Surface Effect Ship (SES) holds promise as a viable and appealing alternative for transferring crew to offshore wind farms and oil platforms due to its superior seakeeping capability, high comfort and speed. A SES is a marine craft with catamaran hull, with flexible stern- and bow rubber -seal system. The air cushion is defined as the enclosed volume between the hull, seals and water plane. Centrifugal lift fans blow air into the air cushion, pressurizing the air cushion that lifts up to 90 % of the vessel weight. Modern SES are also equipped with adjustable vent valves allowing outflow air from the pressurized cushion. By mounting the vent valves on the hull sides, the thrust force coming from the air exiting the vent valves can be seen as an extra actuator on the ship. Using Vent valve to control the ship's position requires an accurate thrust force model. This paper develops two thrust force models and investigates their performance. Both models are compared to computational Fluid Dynamic (CFD) analysis and experimental tests. Results show that both models may be used to estimate the maximum thrust, However, one holds higher promise to be used for control design.

Keywords: Surface Effect Ship, Pressure Force, Dynamic Positioning.

1. INTRODUCTION

A Surface Effect Ship (SES) is a marine craft with catamaran hull, with flexible stern- and bow rubber -seal system. The air cushion is defined as the enclosed volume between the hull, seals and water plane. Centrifugal lift fans blow air into the air cushion, pressurizing the air cushion that lifts up to 85% of the vessel weight. The cushion is sealed off at the bow by so-called finger skirts and the aft is sealed by multiple lobes or bags, as shown in Fig. 1. A detailed description of SESs is given by Butler (1985). The modern SES is equipped with variable vent valves, through which cushion pressure can be controlled by adjusting the air outflow from the cushion. These systems are known as ride control systems (RCS), see Auestad et al. (2015); Hassani et al. (2019); Haukeland et al. (2019). The airflow out of the cushion is controlled by adjusting square butterfly type valves or louvers that is installed in ducts connecting the cushion to the outside atmosphere, such as the ones shown on the scale model in Fig. 2.

In an ongoing research project among SINTEF Ocean, NTNU, and UMOE Mandal, a new SES type are designed with four cushion chambers where each chamber has a regulating vent valve to control the cushion pressure. By mounting the vent valves on the hull sides, the thrust force coming from the air exiting the vent valves can be seen as an extra actuator on the ship. This allows to actively regulate the motions of a SES in sway, heave, roll, pitch, and yaw. Using Vent valve to control the ship's position requires an accurate thrust force model. Furthermore, if a SES is to be fitted with a vent valve control system, being able to estimate the thrust is critical for determining

⋆ This work is supported by the MAROFF-2 programme for research, innovation and sustainability within marine and offshore industries (Project No. 282404).

[1] Corresponding Author.

10.1016/j.ifacol.2019.12.282

the required fans and vent sizing. Also, since the vent valve thrust force depends on the cushion pressure, which is difficult to control, having a realistic thrust model is important for designing the control system.

It was these circle of ideas that motivated us further study the process of thrust generation during the air outflow from the vent valves. This paper investigates two mathematical models for estimating the thrust force from SES vent valves. The models are tested through CFD analysis and scale model experimental tests. This paper develops and compares two thrust force models. Both models are compared to CFD analysis and experimental tests. The results of this article plays a Paramount role in designing control algorithms to regulate sway, heave, roll, pitch, yaw.

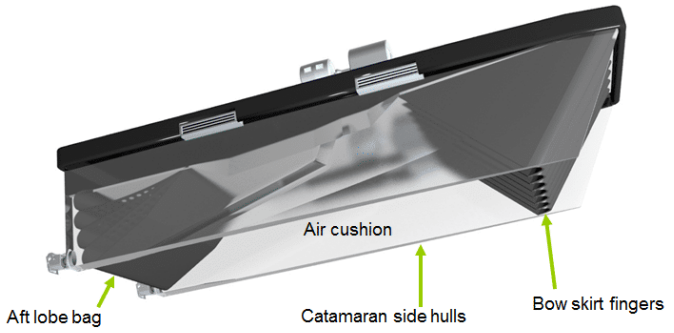

Fig. 1. Surface Effect Ship concept, by courtesy of Umoe Mandal.

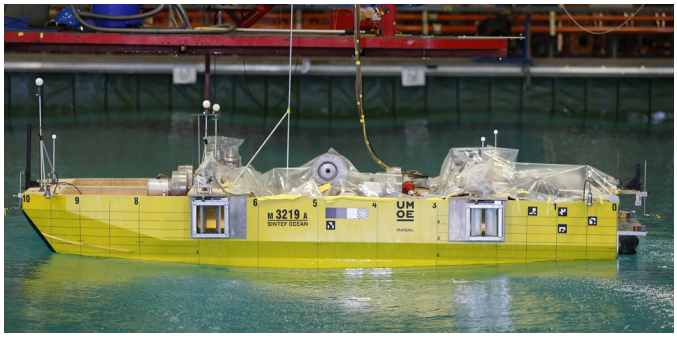

Fig. 2. Scale model B in the ocean basin at SINTEF Ocean.

The rest of the article is organized as follows. Section 2 gives a brief overview of thrust generation during air outflow in SES. In section 3, a short description of two scaled model vent valves, that were used in the experimental testings, are presented. Section 4 provides the key results behind the proposed thrust models through comparison by model test data and CFD simulations. Conclusions and suggestions for future research are summarized in Section 6.

2. THRUST FORCE

2.1 Thrust model 1

To derive the first model for thrust force from the vent valves, consider a vent with a square cross section and a valve consisting of adjustable louvers, as illustrated in Fig. 3. The inlet of the vent valve is connected to the pressurized air cushion in the SES, while the outlet is open to the atmosphere. The flow velocity is assumed to be zero at the inlet, v_c at the center of the valves and the flow exits the vent with velocity v_{out} and volumetric flow rate Q_{out}. The excess pressure or pressure difference between the cushion and atmosphere is p and it is assumed that there is atmospheric pressure at the center of the valve.

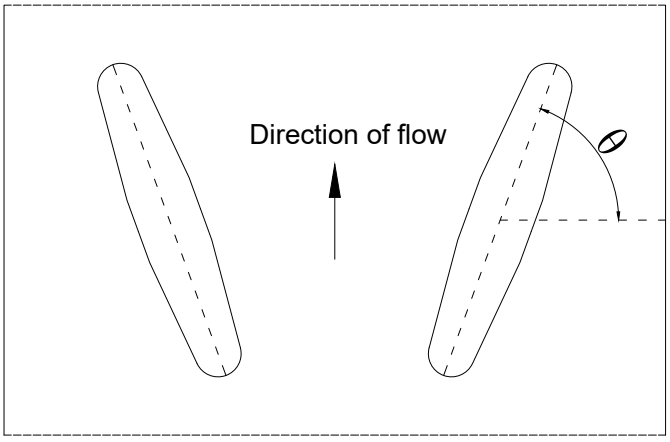

Fig. 3. Top view of vent valve.

From Newton's second law with the assumption of steady state and incompressible flow, the thrust force from a vent valve is

$$f = \frac{d}{dt}(mv) = \rho Q_{out} v_{out} \tag{1}$$

The first thrust model assumes that the valves in the vent are simplified to the projected area as seen along the direction of flow. Bernoulli's principle relates the cushion pressure to the velocity at the center of the valves such that

$$\frac{p}{\rho} = \frac{v_c^2}{2} \tag{2}$$

To account for any losses, the orifice coefficient c_n is introduced such that the velocity at the center of the valves is

$$v_c = c_n \sqrt{\frac{2p}{\rho}} \tag{3}$$

From the velocity at the center of the valves, the volumetric flow rate at the center and consequently at the outlet due to continuity is

$$Q_{out} = c_n \sqrt{\frac{2p}{\rho}} A_L \tag{4}$$

where A_L is the vent valve leakage area.

From continuity and the assumption of incompressible flow

$$v_{out} A_v = Q_{out} \tag{5}$$

where A_v is the vent area, such that the velocity at the outlet in terms of the excess cushion pressure is

$$v_{out} = \frac{A_L}{A_v} c_n \sqrt{\frac{2p}{\rho}} \tag{6}$$

Finally, inserting (6) into Newton's second law, the first model for thrust force from a vent valve is obtained as

$$f_1 = 2 c_n^2 p \frac{A_L^2}{A_v} \tag{7}$$

Since this model is based on flow through an orifice, the leakage area for a square vent valve with side length s and n_l louvers that are s/n_l wide and $\epsilon s/n_l$ thick, may be expressed in terms of the opening angle as

$$\begin{aligned} A_L &= A_v - \left(\frac{s}{n_l}\cos\theta + \frac{\epsilon s}{n_l}\sin\theta\right) s n_l \\ &= (1 - \cos\theta - \epsilon\sin\theta)s^2 \end{aligned} \tag{8}$$

Then,

$$f_1 = 2c_n^2 p s^2 (1 - \cos\theta - \epsilon\sin\theta)^2 \tag{9}$$

The first thrust model is derived based on flow through an orifice. As such, it is highly simplified. However, RCS designs typically use (4) to model the airflow out of the vent valves, see e.g. Kaplan et al. (1981) and Sørensen and Egeland (1995), and Auestad et al. (2015) presents a heave control system that use (4). Details on the mathematical modelling of the coupled vessel and pressure cushion dynamics that is used in the aforementioned work are given by Steen (1993). Although the analysis by Steen is very detailed, the airflow out of the cushion is based on (4) with an orifice coefficient assumed to vary between 0.61 and 1, based on results by P. A. Sullivan (1992).

2.2 Thrust model 2

An alternative approach to determine the velocity exiting a vent valve is to start from the steady flow equation as presented by White (2015),

$$\left(\frac{p}{\rho g} + \frac{\alpha_{out} v^2}{2g} + z\right)_{out} = \left(\frac{p}{\rho g} + \frac{\alpha_{in} v^2}{2g} + z\right)_{in} + h \tag{10}$$

where α is a kinetic energy correction factor which is approximately 1 for turbulent flow. h represents the losses in the system and may be written as the sum of the friction loss between the fluid and the duct h_f and other losses h_m,

$$h = h_f + \sum h_m = \frac{v^2}{2g}\left(f\frac{L}{s} + \sum K\right) \tag{11}$$

In the above equation, f is the Darcy friction factor which is a function of Reynold's number and pipe roughness. L/s is the length to width ratio of the duct and K is a loss coefficient determined from the loss across artifacts such as bends, edges and valves by

$$K = \frac{v_{in}^2 - v_{out}^2}{2g} = \frac{p_{in} - p_{out}}{\rho g} \tag{12}$$

For the vent valve system on a SES, there are losses due to the valve, bends and the contraction from the cushion to the ducts. The loss due to the valve grow almost exponentially with closing angle and approach zero for full opening, depending on the width and shape of the valve (White (2015)). The loss due to the bends depend on the ratio between bend radius and duct width, such that a increasing the radius reduces the loss coefficient. For a smooth pipe with a radius equal to the width, $K_{bend} \approx 0.25$. The loss due to a sudden contraction depends on the contraction ratio and approaches 0.42 as the ratio contraction ratio approaches zero. However, this is assuming sharp edges at the contraction. Thus, except for when the valves are fully open, the valves will dominated the minor losses. The loss for the relevant length to width ratios and frictions factors is very low, typically, $fL/s < 0.05$ and the static pressure loss is also negligible.

For the purpose of deriving a thrust model for varying vent valve angle, the loss coefficient is divided into a valve loss coefficient $K_v(\theta)$ and a constant loss coefficient K_c to account for the other losses in the system such that

$$K(\theta) = K_v(\theta) + K_c \tag{13}$$

Assuming that the flow exits the pipe with velocity v at atmospheric pressure and enters the pipe with zero velocity at pressure $p_{atm} + p$ and that all losses except the valve loss is neglected, (10) reduces to

$$\frac{p}{\rho g} = \frac{v^2}{2g} + \frac{v^2}{2g}K(\theta) \tag{14}$$

such that the outlet velocity is

$$v = \sqrt{\frac{2p}{\rho(1 + K(\theta))}} \tag{15}$$

Inserting into Newton's second law, the second model for thrust force from one vent valve is

$$f_2 = \frac{2p}{(1 + K(\theta))}A_v \tag{16}$$

3. COMPARISON TOOLS

The generated force by vent valves are measured in model scale experiments and calculated using CFD tools. Each approach is brifely presented in this section.

3.1 Model testing

Two scale models have been used to verify the vent valve thrust force. The vents used on model A and B are shown in Figs. 4 and 2, respectively. Both of the models are built in scale to one of Umoe Mandal's SESs and are complete with vent valves, fans, finger skirt and lobe bag. The experimental testing has been performed at SINTEF Ocean's laboratories.

The difference between the two models is mainly the vent valves and the how the tests were performed. Model A has one vent valve on each side and the valves in the vents are three thin plates. Model B has two vent valves on each side and the valves in the vents are thicker, but more rounded. Also, the vent valves model B has a better seal when the valves are closed and the testing of model A was performed with the model attached to a fixed arm, through a load cell, while the second model was floating freely, but connected to soft springs through load cells.

From the measured pressure p and force F obtained from the testing, the orifice coefficient and loss coefficient have been calculated as

$$c_n = \sqrt{F\frac{A_v}{2pA_L^2}} \tag{17}$$

and

$$K = \frac{2p}{F}A_v - 1 \tag{18}$$

respectively.

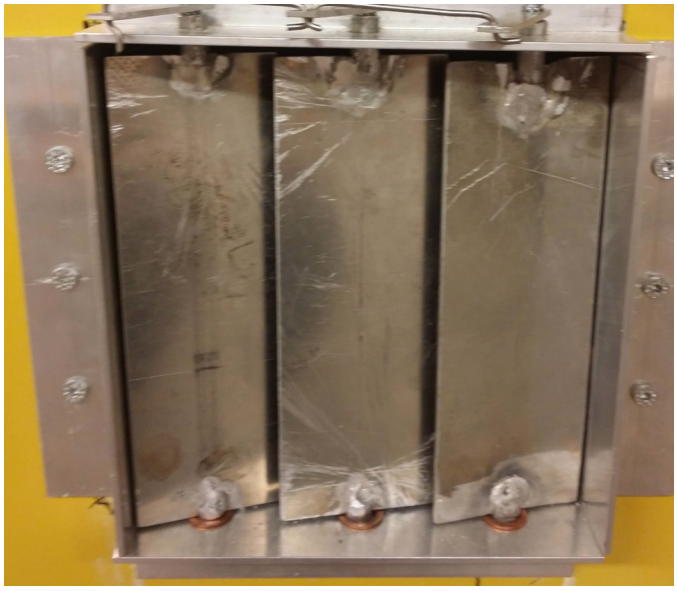

Fig. 4. Vent valves on scale model A.

Scale model B were fitted with a rigid wall along the centerline which divided the pressure cushion at large drafts. Since dividing the cushion along the center induces a roll angle and less pressure is provided for sway force, the test were performed at relatively high pressures. This lead to significant air leakage under the starboard hull at low valve angles. Also, during the tests, the valves were only allowed to go to a maximum opening angle of approximately 75°. Consequently, most of the results presented are from scale model A and the CFD analysis.

3.2 CFD Analysis

CFD analysis of a vent valve system with valves modelled according to scale model B has been performed in Autodesk CFD. Analysis for various vent valve openings have been performed with fixed pressure as boundary conditions on the aft and forward cushion sides and zero pressure on the outlet. The pressure used for each vent valve opening have been determined assuming frictionless flow out of the cushion. All analysis have been performed assuming steady state and incompressible flow.

From the outlet pressure p and velocity v obtained from the CFD analysis, the the orifice coefficient and loss coefficient have been calculated as

$$c_n = v\sqrt{\frac{\rho}{2p}}\frac{A_v}{A_L} \tag{19}$$

and

$$K = \frac{2p}{\rho v^2} - 1 \tag{20}$$

respectively.

4. RESULTS

This section summarises results of both model test and CFD analysis.

4.1 Orifice coefficient c_n

The calculated orifice coefficient from the CFD analysis and experimental tests are shown in Fig. 5. For valve angles above 70°, the orifice coefficient is between 0.7 and 1, which is as expected and in line with the values given by Faltinsen (2012). However, for lower angles, the orifice coefficient increase beyond 1. From the definition of c_n, it is not physically possible for it to exceed 1, since this would mean that pressure is added to the system, not lost. This is likely because the valves change the direction of the flow, which does not happen with flow through an orifice. Also, the orifice coefficients from scale model A is higher for most of opening angles. By the previous reasoning this makes sense since the valves on model A turn in the same direction. This causes the flow to deviate more from the assumed orifice flow.

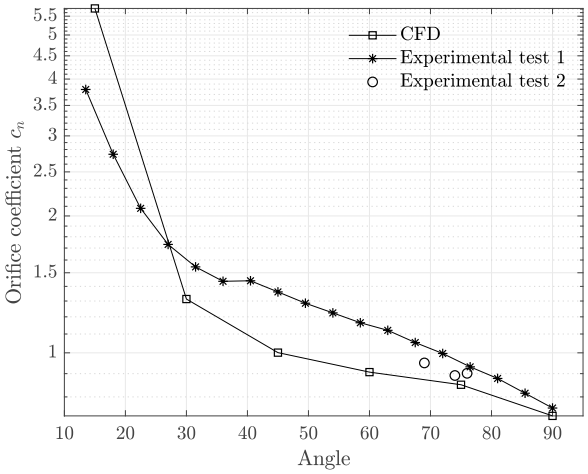

Fig. 5. Orifice coefficient obtained from CFD analysis and experimental test.

4.2 Loss coefficient K

The calculated loss coefficient from the CFD analysis and experimental tests are shown in Fig. 6. The loss coefficients are not far from having an exponential relationship with valve angle. The valve used in the CFD analysis is modelled based on the valve on model B and these loss coefficients match quite well. The loss coefficient for the vent valve on model A is lower, especially at low opening angles. This is likely because the valves on model A do not seals the vent at zero opening and that the louvers used in each valve are much thinner than the ones used on model B and in the CFD analysis.

The loss coefficients shown in 6 are for the complete vent valve system. For the CFD analysis it is possible to find the valve loss coefficient by simulating the flow without the valve. The loss coefficient obtained then is approximately 1. Since the total loss coefficient of the first model is very low at full opening (0.86), it is assumed that the loss coefficient of model A without valve is 0.76.

When subtracting the constant loss coefficient, the valve loss coefficient is obtained. These values have been fitted to an equation on the form

$$\frac{1}{K_v} = \alpha \exp\left(\frac{\pi\beta\theta}{180}\right) \tag{21}$$

where θ is measured in degrees and α and β are parameters. The calculated and fitted values for the valve loss coefficient are shown in Fig. 7.

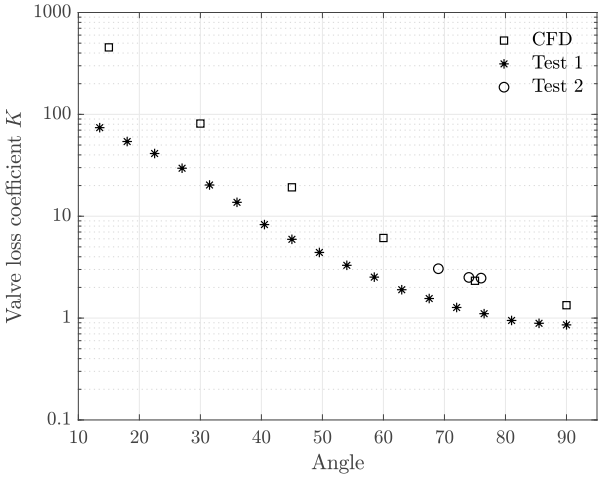

Fig. 6. Loss coefficient K for valve opening angle.

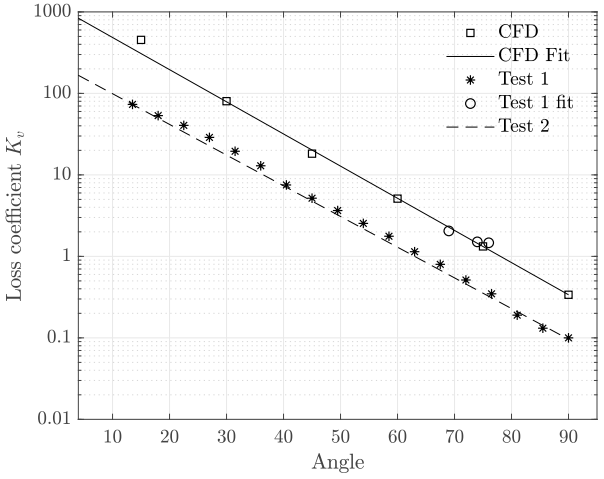

Fig. 7. Valve loss coefficient K_v for valve opening angle.

4.3 Vent valve force

The vent valve force obtained from the CFD analysis is compared with thrust model 1 (9) and thrust model 2 (16) in Fig. 8. Fig. 9 shows the two models compared with the force obtained from the experimental test performed on scale model A. Assuming an orifice coefficient of 0.8, the first thrust model is not very far off from the CFD analysis, but is quite poor compared to scale model A, except at high opening angles. As mentioned previously, this is likely because the valve used for the CFD analysis creates a flow pattern more similar to orifice flow than that of the vent valve on model A.

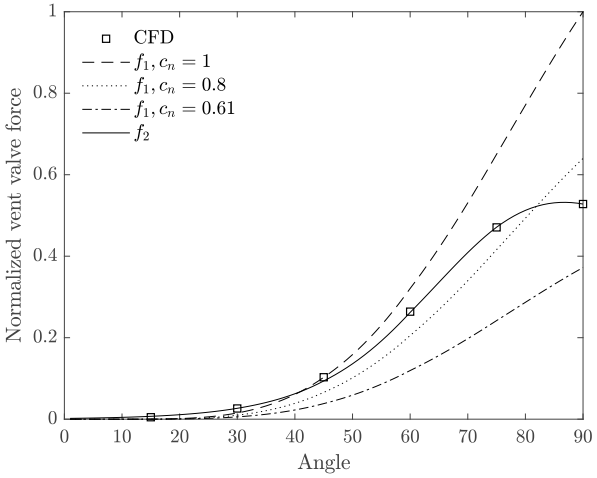

Fig. 8. Vent valve force from CFD compared with thrust model 1 and 2.

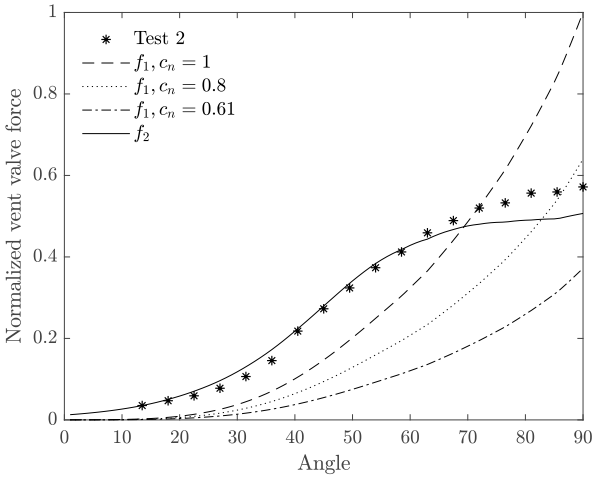

Fig. 9. Vent valve force from CFD compared with thrust model 1 and 2.

5. DESIGN OF VENT VALVE DP SYSTEMS

During the design phase for a SES with DP capability, the main concern with regards to the DP system is the required installed thrust capacity. When installing thrusters, this is quite simple, as the manufacturer provide thrust characteristics and power rating. However, the vent valve thrust is a combination of the fans installed, vent sizes and geometry, and the type of valve used in the vent. Thus, during initial design the main concern is to be able to estimate the thrust produced by the vents. To this end, the following section derives an analytic expression to estimate the force from a vent valve system.

The fan thrust characteristics is provided by the manufacturers. The airflow into the cushion from one fan may be modelled on the form

$$q_{in} = a q_{max} \left(\frac{p_{max} - p}{p_{max}}\right)^{1/b} \tag{22}$$

where q_{max} and p_{max} are design operational limits of the fan and a and b are used to fit (22) to the fan thrust

characteristics provided by the manufacturer. Using the second thrust model, the airflow out of a vent is

$$q_{out} = \sqrt{\frac{2p}{\rho(1+K(\theta))}} A_v \tag{23}$$

Now, consider a SES with n_v valves on port and starboard side. The total airflow out is

$$Q_{out} = n_v q_{out} \tag{24}$$

and the total airflow in from n_f fans, assuming $a = 1$ and $b = 2$, is

$$Q_{in} = n_f q_{max} \sqrt{\frac{p_{max} - p}{p_{max}}} \tag{25}$$

By equating the airflow out (24) and airflow in (25) an analytic expression for the cushion pressure is obtained as

$$p = \frac{n_f^2 q_{max}^2 p_{max} \rho (1 + K(\theta))}{2 n_v^2 A_v^2 p_{max} + n_f^2 q_{max}^2 \rho (1 + K(\theta))} \tag{26}$$

The total force in sway now becomes

$$F_{sway} = 2 n_v A_v \frac{n_f^2 q_{max}^2 p_{max} \rho}{2 n_v^2 A_v^2 p_{max} + n_f^2 q_{max}^2 \rho (1 + K(\theta))} \tag{27}$$

The above equation can be used in the design phase of a vent valve DP system. For example, the optimal vent area at maximum vent valve opening may be found by

$$\frac{\partial F_{sway}}{\partial A_v} = 0 \tag{28}$$

which gives

$$A_{v,optimal} = \frac{n_f q_{max}}{n_v p_{max}} \sqrt{\frac{\rho(1 + K(90))}{2}} \tag{29}$$

As an example, consider a SES with vent valves on port and starboard side and 6 fans with design limits $p_{max} = 10000$Pa and $q_{max} = 100\text{m}^3$. The maximum sway force when installing 2 or 4 vent valves on each side is shown in Fig. 10 for varying vent size.

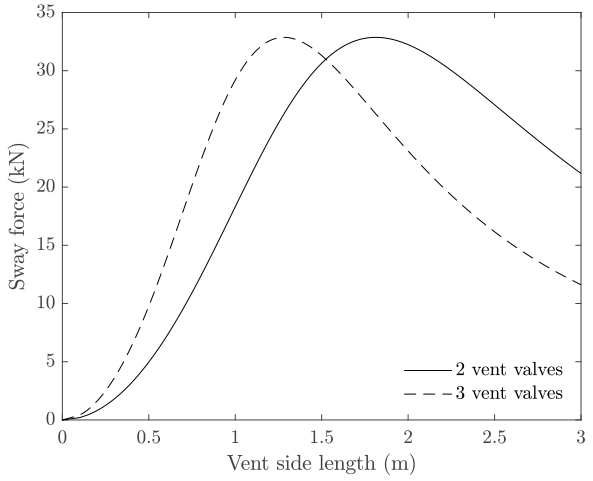

Fig. 10. Maximum sway force when installing 2 or 4 vent valves on each side.

6. CONCLUSION

In this article two thrust models were developed for Vent Valves in surface Effect Ships. Both thrust models provide a practical estimate of the thrust force from a vent valve at maximum valve opening, assuming an orifice coefficient of 0.8 for the first thrust model.

The first model only provides an accurate thrust force estimate when the valve is almost completely open. However, using the second thrust model, one can produce a good predictions of thrust force. The second model relies on valve loss coefficient data, but this is usually supplied by the valve manufacturer. The results show that in lack of valve data, a simple CFD analysis may be used to find the valve loss coefficients.

REFERENCES

Auestad, Ø.F., Gravdahl, J.T., Perez, T., Sørensen, A.J., and Espeland, T.H. (2015). Boarding control system for improved accessibility to offshore wind turbines: Full-scale testing. *Control Engineering Practice*, 45, 207–218. doi:10.1016/j.conengprac.2015.09.016.

Butler, E.A. (1985). The surface effect ship. *Naval Engineers Journal*, 97(2), 200–253. doi:10.1111/j.1559-3584.1985.tb03399.x.

Faltinsen, O.M. (2012). *Hydrodynamics of High-Speed Marine Vehicles*. CAMBRIDGE UNIV PR.

Hassani, V., Fjellvang, S., and Auestad, .F. (2019). Adaptive boarding control system in surface effect ships. In *Proc. of the 17th European Control Conference (ECC 2019)*. Naples, Italy.

Haukeland, O.M., Hassani, V., and Auestad, .F. (2019). Surface effect ship with four air cushions, part ii: Roll and pitch damping. In *Proc. of the 12th IFAC Conference on Control Applications in Marine Systems, Robotics, and Vehicles (CAMS 2019)*. Daejeon, South Korea.

Kaplan, P., Bentson, J., and Davis, S. (1981). Dynamics and hydrodynamics of surface-effect ships. *SNAME Transactions*, 89, 211–247.

P. A. Sullivan, F. Gosselin, M.J.H. (1992). Dynamic response of an air cushion lift fan. In *Intersociety High Performance Marine Vehicle Conference and Exhibit*.

Sørensen, A. and Egeland, O. (1995). Design of ride control system for surface effect ships using dissipative control. *Automatica*, 31(2), 183–199. doi:10.1016/0005-1098(94)00090-6.

Steen, S. (1993). *Cobblestone Effect on SES*. Norges Tekniske Hgskole.

White, F.M. (2015). *Fluid Mechanics*. McGraw-Hill Education - Europe.